FUSION ENERGY DIVISION LIBRARY

ORNL/SUB-33200/4

cy. 23

HUGHES

HUGHES AIRCRAFT COMPANY

ELECTRON DYNAMICS DIVISION

OAK RIDGE NATIONAL LABORATORY LIBRARIES

3 4456 0536817 0

# DEVELOPMENT PROGRAM FOR A 200 kW, CW GYROTRON

J. J. Tancredi, M. Caplan, J. J. Sandoval, W. Weiss

## QUARTERLY REPORT NO. 4
## APRIL THROUGH JUNE 1980

Contract No. W-7405-ENG-26

FUSION ENERGY DIVISION LIBRARY

NOV 6 1980

Prepared by

HUGHES AIRCRAFT COMPANY
Electron Dynamics Division
3100 West Lomita Boulevard
Torrance, California 90509

for
OAK RIDGE NATIONAL LABORATORY
Oak Ridge, Tennessee 37830
operated by
UNION CARBIDE CORPORATION
for the
DEPARTMENT OF ENERGY

This report was prepared as an account of work sponsored by an agency of the United States Government. Neither the United States Government nor any agency thereof, nor any of their employees, contractors, subcontractors, or their employees, makes any warranty, express or implied, nor assumes any legal liability or responsibility for any third party's use or the results of such use of any information, apparatus, product or process disclosed in this report, nor represents that its use by such third party would not infringe privately owned rights.

ORNL/SUB–33200/4

HUGHES

HUGHES AIRCRAFT COMPANY

ELECTRON DYNAMICS DIVISION

# DEVELOPMENT PROGRAM FOR A 200 kW, CW GYROTRON

J. J. Tancredi, M. Caplan, J. J. Sandoval, W.Weiss

## QUARTERLY REPORT NO. 4
## APRIL THROUGH JUNE 1980

Contract No. W-7405-ENG-26

Prepared by

HUGHES AIRCRAFT COMPANY
Electron Dynamics Division
3100 West Lomita Boulevard
Torrance, California 90509

for
OAK RIDGE NATIONAL LABORATORY
Oak Ridge, Tennessee 37830
operated by
UNION CARBIDE CORPORATION
for the
DEPARTMENT OF ENERGY

TABLE OF CONTENTS


| Section | | Page |
|---|---|---|
| I. | INTRODUCTION | 1-1 |
| II. | PROGRESS | 2-1 |
| | 2.1 General | 2-1 |
| | 2.2 Magnetron Injection Gun | 2-1 |
| | 2.3 Superconducting Solenoid | 2-5 |
| | 2.4 RF Circuit Design | 2-5 |
| | 2.5 Collector Design | 2-9 |
| | 2.6 Taper Design | 2-12 |
| | 2.7 Tube Layout | 2-27 |
| | 2.8 Power Supplies | 2-27 |
| III. | SCHEDULE | 3-1 |
| IV. | REFERENCES | 4-1 |

LIST OF ILLUSTRATIONS


| Figure | | Page |
|---|---|---|
| 1-1 | Schematic of gyrotron oscillator showing applied magnetic field and the rf field and gain in the cavity. | 1-3 |
| 2.2-1 | Final magnetron injection gun and magnetic field configurations. | 2-2 |
| 2.2-2 | Gyrotron gun assembly. | 2-4 |
| 2.3-1 | Axial magnetic field for ORNL 60 GHz gyrotron. | 2-6 |
| 2.3-2 | Solenoid coil configuration to produce the axial field of Figure 2.3-1 | 2-7 |
| 2.5-1 | Computer plot of the electron beam in $TE_{02}$ cavity. | 2-10 |
| 2.5-2 | Graphic plotter output of an electron beam RF modulated by a cavity, and impacting on the collector walls. | 2-11 |
| 2.5-3 | Trajectory plot of an unmodulated electron beam traversing the cavity region and impacting on the collector walls (for the case of a tapered magnetic field over the cavity). | 2-13 |
| 2.5-4 | Averaged power dissipation on the collector, for the trajectory plot of Figure 2.5-3. | 2-14 |
| 2.6-1 | Unger's raised cosine taper for 55 GHz (Reference 2). | 2-16 |
| 2.6-2 | $TE_{01}$ raised cosine tapper for 94 GHz gyrotron amplifier, with ≈ 30 dB suppression of the $TE_{02}$ mode. | 2-18 |
| 2.6-3 | Linear taper for the ORNL 60 GHz gyrotron. | 2-19 |
| 2.6-4 | Raised cosine taper for the ORNL gyrotron, with the $TE_{01}$ mode suppressed 17.3 dB. | 2-21 |
| 2.6-5 | "Two-arc" taper for 20 dB $TE_{01}$ mode suppression in the ORNL gyrotron. | 2-22 |

LIST OF ILLUSTRATIONS (CONTINUED)


| Figure | | Page |
|---|---|---|
| 2.6-6 | A "two arc/linear" taper of 40 cm length. | 2-23 |
| 2.6-7 | "Two arc" "down" taper of 30 cm length. | 2-24 |
| 2.6-8 | A modified "two arc" taper of 30 cm length. | 2-25 |
| 2.6-9 | Combined "up" taper, collector region, and "down" taper with 17 dB overall suppression of the $TE_{01}$ mode. | 2-26 |
| 2.7-1 | Preliminary 917H gyrotron layout for ORNL. | 2-28 |

# I. INTRODUCTION

The objective of this program is the design and development of a millimeter-wave device to produce 200 kW of continuous-wave power at 60 GHz. The device, which will be a gyrotron oscillator, will be compatible with power delivery to an electron-cyclotron plasma. Smooth control of rf power output over a 17 dB range is required, and the device should be capable of operation into a severe time-varying rf load mismatch.

The technical baselines for the gyrotron and the associated power supply are shown in Table I. In the gyrotron, which is shown schematically in Figure 1-1, the electrons are formed into a hollow beam by a magnetron-injection electron gun with a considerable amount of their energy in rotation. A gradually rising magnetic field compresses the beam in diameter and at the same time increases the orbital energy according to the theory of adiabatic invariants until approximately 2/3 of the beam energy is in rotation and the rotational frequency is 60 GHz; at this point the magnetic field becomes uniform and the beam enters a quasi-optical open cavity where the spinning electrons interact with the eigen mode of the cavity. The rf energy builds up at the expense of the rotational energy of the dc beam. The spent beam enters the region of decreasing magnetic field, undergoes decompression and impinges on the collector. The latter also functions as the output waveguide. In order to handle the power in the spent beam and the power dissipation in the window, the output waveguide tapers up from the cavity diameter to an appropriate value.

The duration of the program is 36 months, to encompass the building and test of up to twelve devices. The magetron injection gun is well understood and allows the use of the extraction anode (as well as

TABLE I

| | |
|---|---|
| **The Gyrotron** | |
| Frequency | 60 GHz |
| Power out | 200 kW RF |
| Electronic efficiency | 35% |
| Beam voltage | 80 kV |
| Beam current | 7.0 A |
| Modulation voltage | 23 kV |
| Magnetic field | 23.0 kG |
| Transverse to longitudinal velocity ratio | 1.5 - 2.0 |
| Cathode Loading | 4.0 $A/cm^2$ |
| Cathode radius | 0.60 cm |
| **The Power Supply** | |
| Voltage rating | 100 kV dc |
| Current rating | 10 A |
| Anode supply voltage | 0-35 kV dc |
| Anode supply current | <20.0 mA |
| Heater supply voltage | 0-15 V, ac |
| Heater supply current | 15 A |
| Operating Modes: | |
| 1. | 10 μs pulse length |
| 2. | 1 ms - 100 ms pulse length |
| 3. | 30 s to cw |

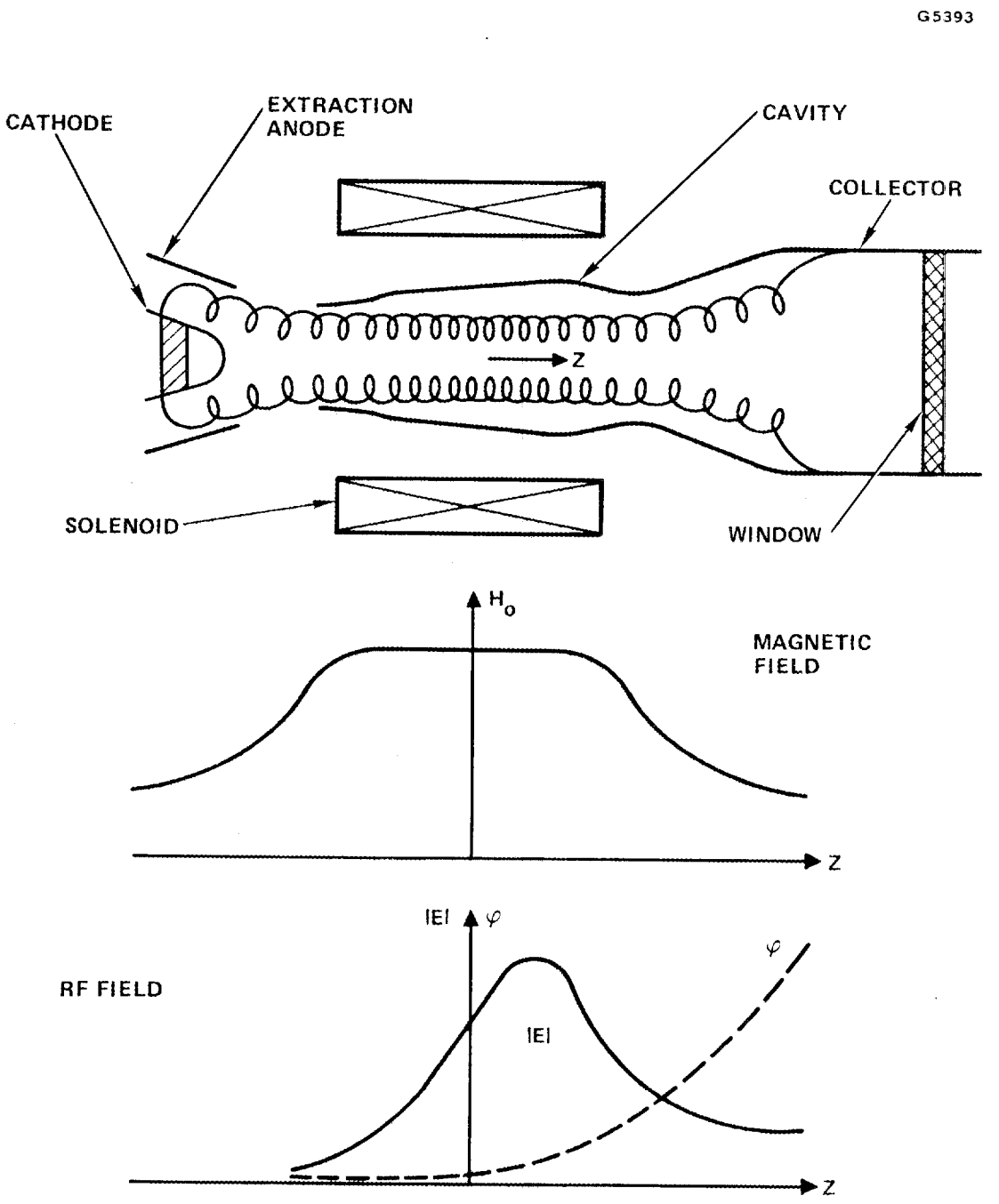


Figure 1-1 Schematic of gyrotron oscillator showing applied magnetic field and the rf field and gain in the cavity.

cathode temperature variation) to vary the rf power out. The collector has to be able to dissipate over 550 kW in undepressed operation. Fabrication and processing of prototype devices will proceed in parallel.

During this reporting period work was continued on a number of design tasks, including the magnetron injection gun, solenoid, rf circuit, collector, taper, and power supply. These activities are detailed in Section II of this report.

# II. PROGRESS

## 2.1 GENERAL

During this report period, effort was applied to the following design tasks:

- Magnetron Injection Gun
- Superconducting Solenoid
- RF Circuit
- Collector
- Tapers
- Tube Layout
- Power Supply

## 2.2 MAGNETRON INJECTION GUN

The design of the magnetron injection gun was finalized electrically and mechanically. Figure 2.2-1 shows a beam trajectory plot over four contiguous frames, from the cathode to the cavity, which is located 30 cm from the cathode snout. This figure also shows the magnetic field slope over the same region. By judicious variation of the magnetic field, an average transverse velocity spread of ±1.05% was computed in the cavity region, with $v_\perp/v_z = 2.35$.

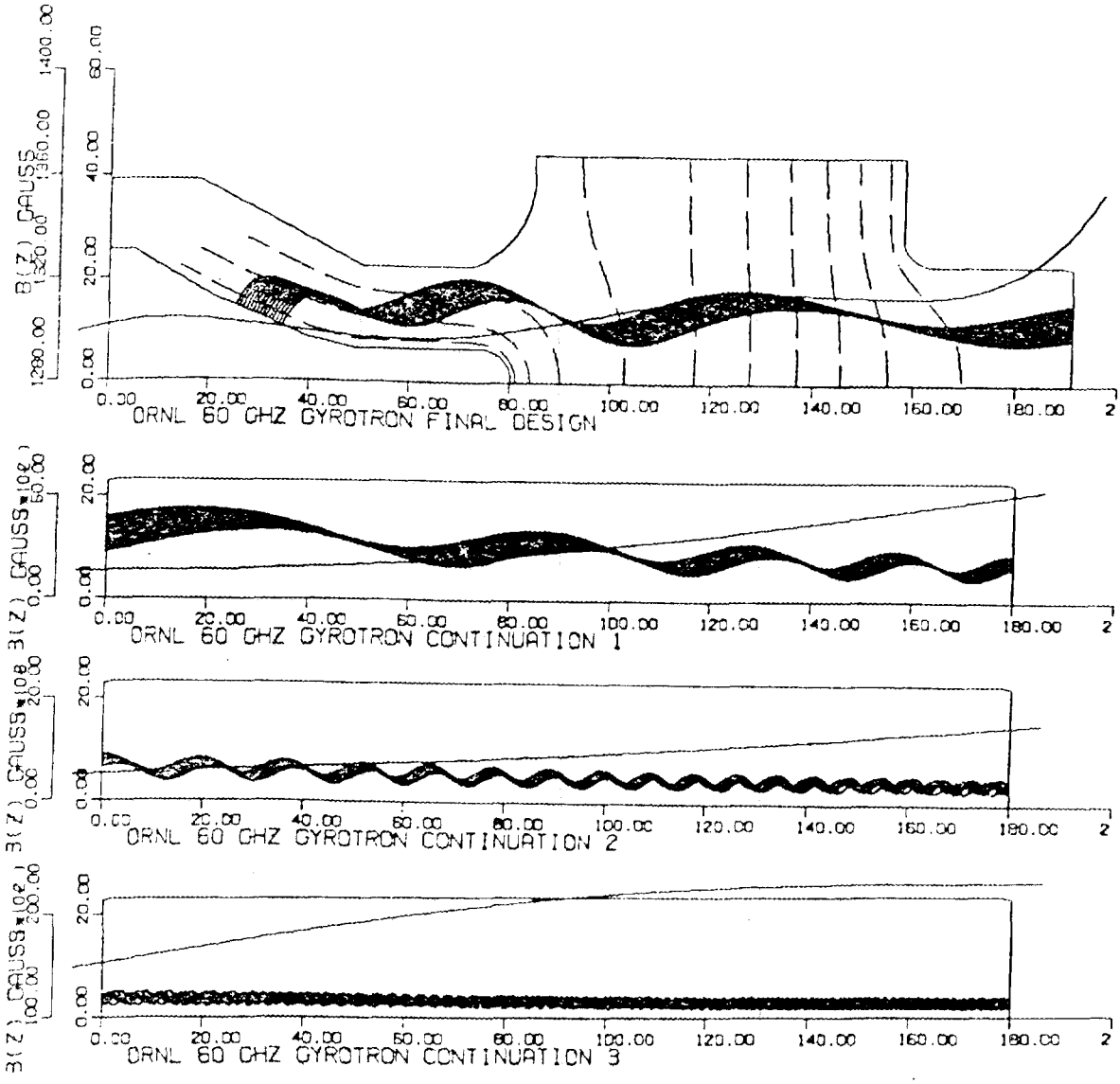


Figure 2.2-1 Final magnetron injection gun and magnetic field configurations.

This value of $\alpha$ ( = $v_\perp/v_Z$) exceeds the design value of $\alpha = 1.5$ and implies that this gun design is working much better than expected. Since efficiency is directly related to the amount of energy in rotation, efficiencies greater than 40% can be anticipated.

However, these excellent results must be tempered by the realization that the trajectory program does not include the effects of cathode macrostructure, nor the effects of thermal electron velocity distribution at the cathode. It is anticipated that these effects will add several percent to the transverse velocity spread.

The gun mechanical design is being centered on the use of existing ceramic gun stem assemblies, in order to expedite the construction of the first tube. Figure 2.2-2 shows the stem assembly for the present tube. The maximum OD of the assembly shown is 3.5". It is proposed to enclose the gun in a grounded can of 4.7" ID and fill the space with FC-75 flurocarbon liquid. FC-75 has a dielectric strength of 400V/mil, which should be sufficient to hold off voltages exceeding 200 kV. FC-75 is the same liquid which will cool the surfaces of the double disc windows.

Figure 2.2-2 also shows that the gun end of the tube contains a pump-out tubulation. This is an auxillary pump-out port to the main manifold located at the collector end of the tube. After pinchoff, normal tube operation will subject the gun area to considerable quantities of deleterious gas. This gas will be difficult to pump through the cavity drift tube because of its small size and high pumping impedance. It is therefore proposed to use a 2 liter/second ion pump mounted directly off the gun pump-out tubulation. This location will result in fast, uninhibited pumping speed of the gun region.

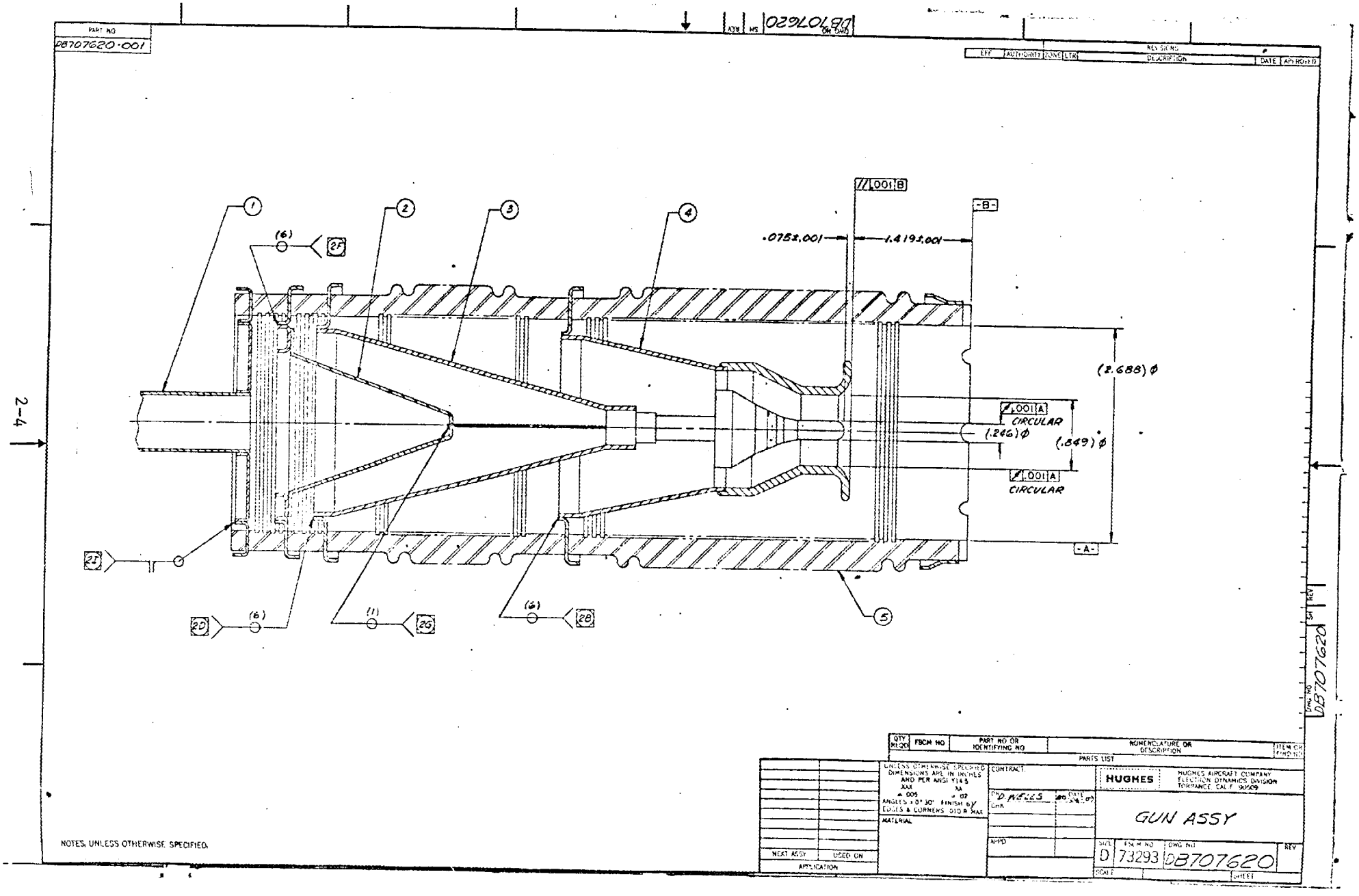


Figure 2.2-2 Gyrotron gun assembly.

## 2.3 SUPERCONDUCTING SOLENOID

The magnetic field required to achieve the results of Section 2.2 is reproduced with more clarity in Figure 2.3-1. In order to produce the desired field variation with distance, and in order to maintain versatility through the gyrotron development cycle, eight independent coils are used. These coils permit cavity magnetic field tapering and shifting of the cathode or cavity regions a distance of ±1 cm, independently from one another.

In a deliverable solenoid to be employed in a plasma heating application, the coils would be connected so that only three supplies would be required. Alternatively, as the gyrotron design becomes finalized, the actual number of coils could be reduced.

The required magnetic field was evolved through existing Hughes computer codes which mathematically assume all the solenoid current passes through a coil of one turn. The location of the coils for the field described by Figure 2.3-1 is shown in Figure 2.3-2.

The required current density for each coil is given in Table 2.3-1. These current densities are relatively conservative and they should permit attainment of 23 kG without training of the Nb Ti superconductor.

The warm bore ID is set at 12.7 cm (5"). An estimated ID for the coils is 17.0 cm, which encloses a vacuum, nitrogen and helium barrier, and the coil bobbin thickness. Toward the end of this report period, a technical specification for the solenoid was written and issued for bid.

## 2.4 RF CIRCUIT DESIGN

The cavity computer program, which was discussed in the last report,[1] was used to evaluate many cavity designs. From these computer runs,

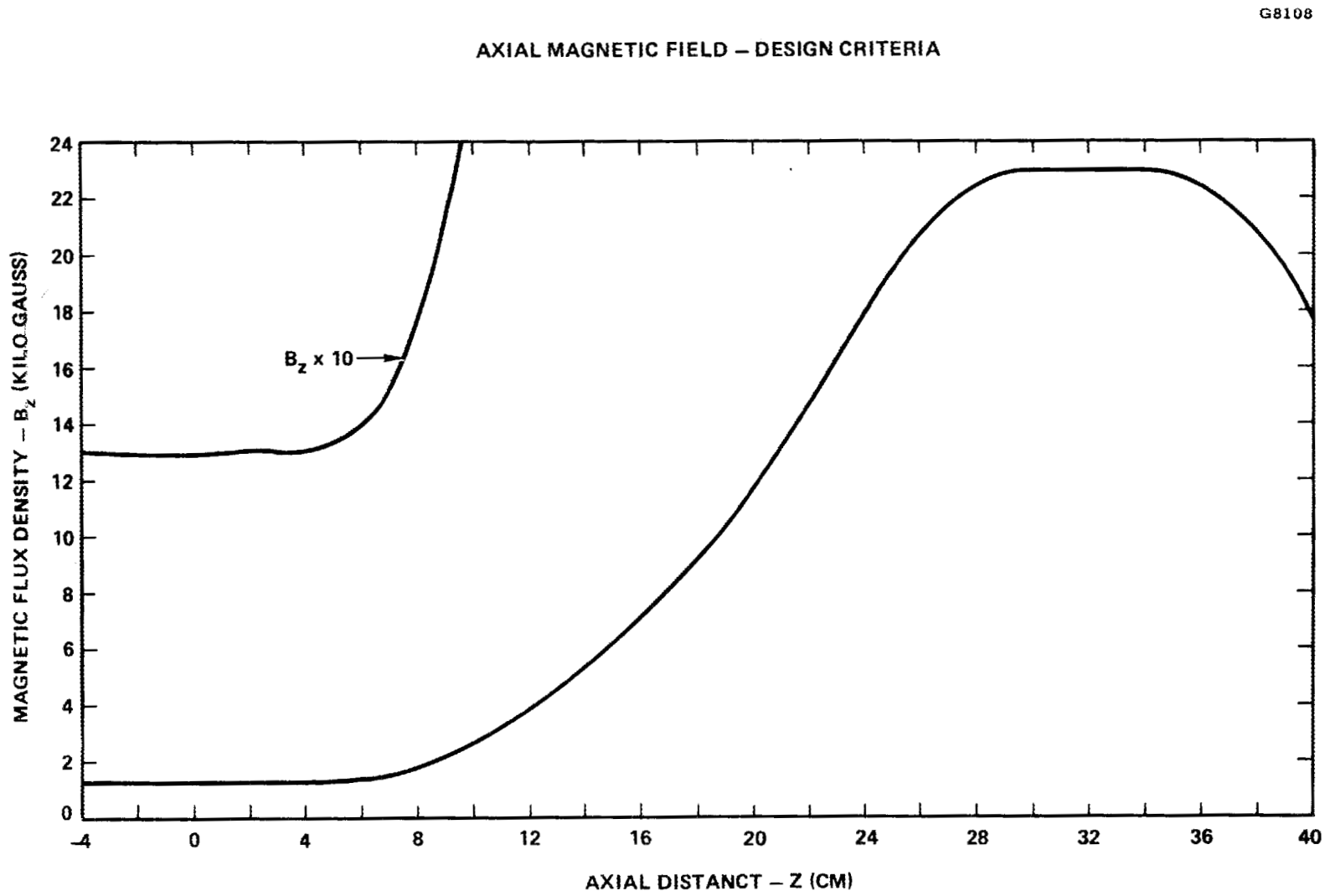


Figure 2.3-1 Axial magnetic field for ORNL 60 GHz gyrotron.

G8109

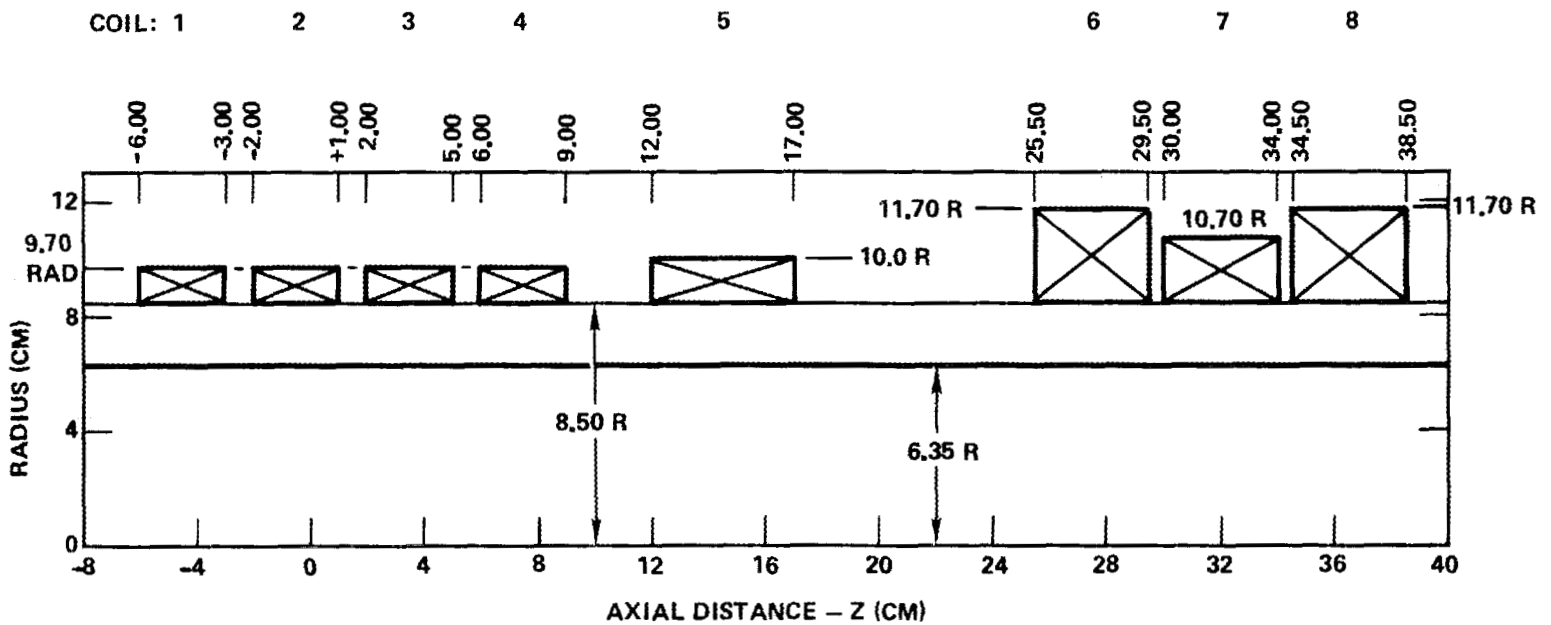


Figure 2.3-2 Solenoid coil configuration to produce the axial field of Figure 2.3-1.

TABLE 2.3-1

ELECTRICAL PARAMETERS FOR MODEL COIL

| Coil No. | Current Density (A/cm$^2$) * | Current (Amps) | Axial Field (Gauss) ** |
|---|---|---|---|
| 1 | 3937 | 14174.2 | 967.0 |
| 2 | -3173 | -11421.6 | -779.2 |
| 3 | 6024 | 21684.6 | 1479.3 |
| 4 | -9449 | -34015.0 | -2320.5 |
| 5 | 3113 | 23350.8 | 1534.0 |
| 6 | 23237 | 297437.4 | 18290.6 |
| 7 | -9514 | -83729.7 | -5386.1 |
| 8 | 23489 | 300655.8 | 18488.6 |

*Assumes coil formed from single conductor of one turn, whose cross-section is the size of the coil; no insulation.

**Field produced on axis, at the center of each coil.

cold test cavities were configured of those cavities which provide the greatest promise. Initial cold testing will be implemented at 10 GHz in order to verify the results of the computer code.

The cold test cavities were fabricated and were received near the end of this report period. Cold testing will be completed by mid August.

## 2.5 COLLECTOR DESIGN

An axisymmetric collector approach is being pursued. As such, the design must compromise adequate collector surface area at a reasonable diameter which does not introduce too many undesirable modes. The collector approach presently being evaluated uses a 3.5" diameter in the collection region.

The results of the magnetron injection gun computer program are used as input data to the cavity. The cavity large signal analysis is next run to introduce a desired amount of beam modulation. This can be seen in Figure 2.5-1, which illustrates the beam and cavity region. The cavity used for this plot has a slight taper on the input side (left side), and a $30^{\circ}$ horn at its output. The beam enters in random phase through its cycloidal path. Under the influence of RF, phase bunching of the beam occurs. This can be seen very clearly as the beam leaves the cavity horn; the cycloidal motion of each trajectory approaches the same phase and the larmor radius appears to decrease.

For collector design, the beam is allowed to continue traveling under the influence of the magnetic field. Figure 2.5-2 shows the graphic plotter output for the beam in the cavity-collector region, under conditions of full RF. The spent beam is collected over a length of approximately 25 cm, inside the 8.89 cm (3.5") diameter collector, or a surface area of approximately 700 $cm^2$. The estimated power density

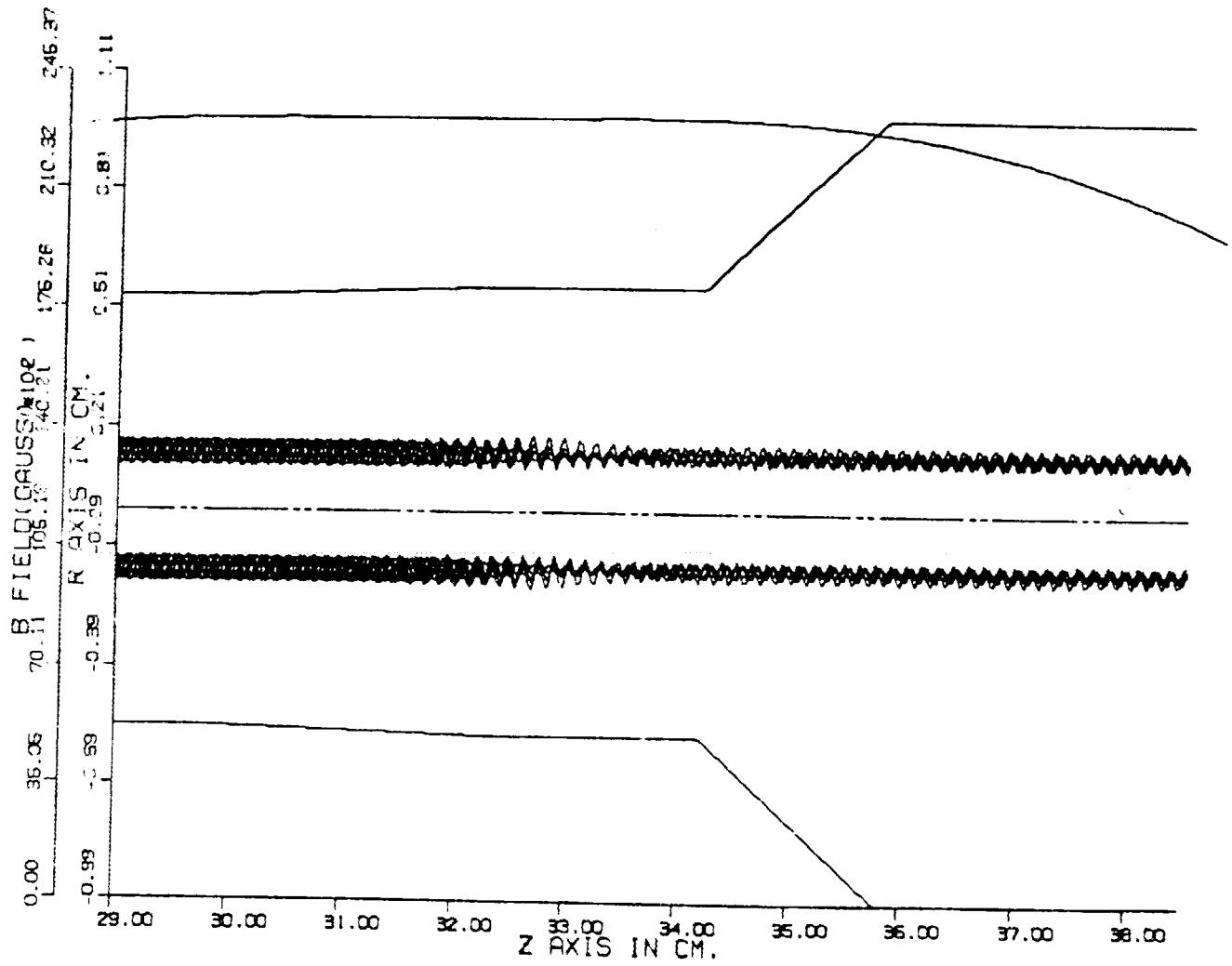


Figure 2.5-1 Computer plot of the electron beam in a $TE_{02}$ cavity.

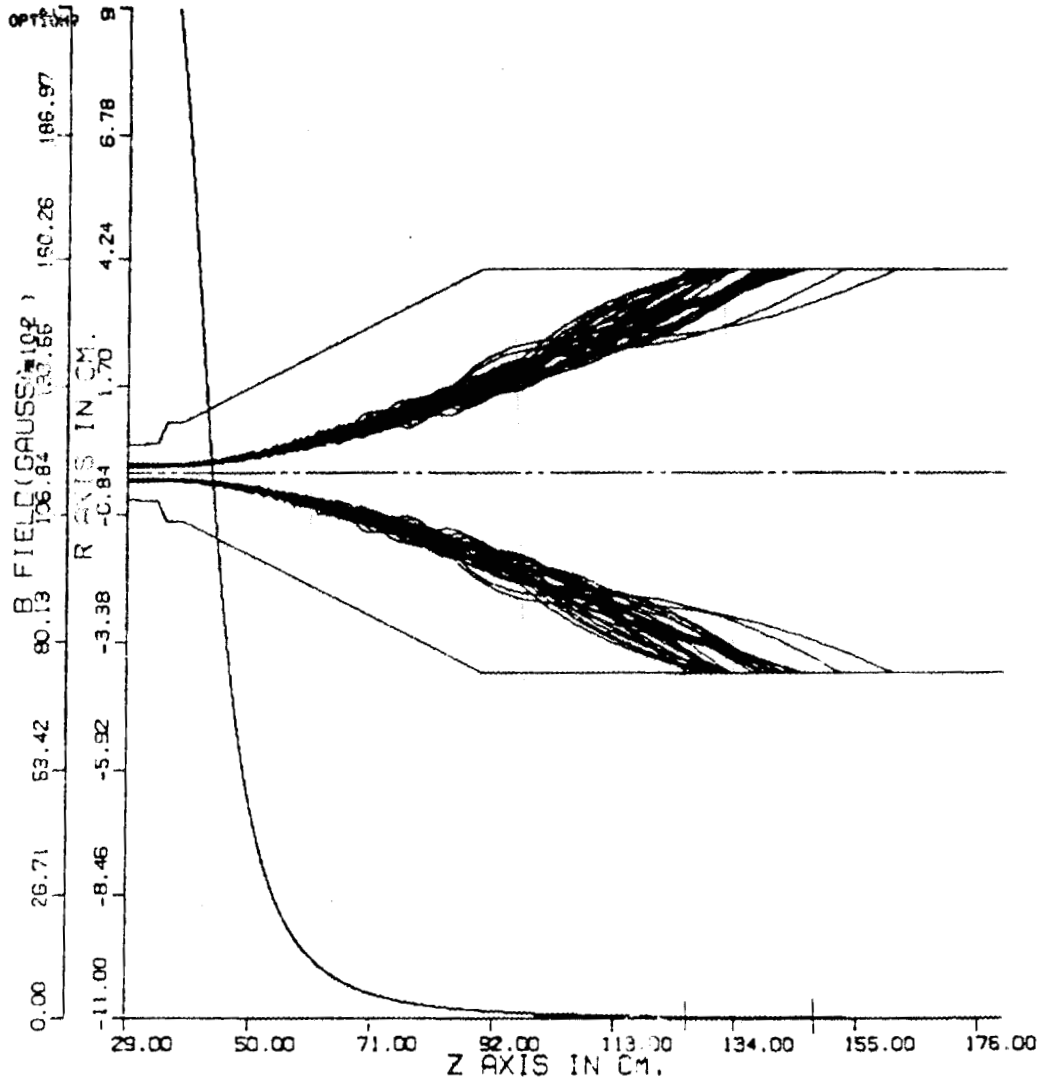


Figure 2.5-2 Graphic plotter output of an electron beam RF modulated by a cavity, and impacting on the collector walls.

for this full CW case would be a reasonable 520 $W/cm^2$. This estimate excludes the two longer rays which are collected farther down the tube, and assumes 200 kW of the 560 kW beam power is converted to RF.

When the gyrotron is not oscillating, with full CW beam conditions, a worst-case power dissipation situation arises. Figure 2.5-3 is a recorder output trajectory plot of this case, including a tapered magnetic field over the cavity. The effect of the magnetic field taper, which is intended to enhance efficiency, is to push the beam farther down the axis. The "averaged" power density for this beam on the collector wall is shown in Figure 2.5-4. This figure was derived using 10% incremental lengths over which the beam power is averaged.

The maximum power density indicated by Figure 2.5-4 is 790 $W/cm^2$, which occurs at two places over the length of the collector. This power density can readily be water-cooled with existing technology.

Note, that no auxillary solenoid coils are required over the collector to assist in spreading the beam. In order to confirm our computer-aided techniques, the first tube will be constructed with a relatively thin wall collector and tested under low duty pulsed conditions. By using photographic plates around the outside of the collector, X-rays emitted by the beam striking the collector wall should reveal the actual collector power density. In the event that auxillary coils may be required, Hughes EDD has an in-house capability to wind conventional room-temperature solenoids without introducing a long program delay.

## 2.6 TAPER DESIGN

The gyrotron being developed employs an axisymmetric collector. As such, the RF output and electron beam travel together into the collector. The collector diameter has temporarily been fixed at 8.89 cm (3.5"), while

Figure 2.5-3 Trajectory plot of an unmodulated electron beam traversing the cavity region and impacting on the collector walls (for the case of a tapered magnetic field over the cavity).

(Figure 2.5-3 appears as a foldout on following page.)

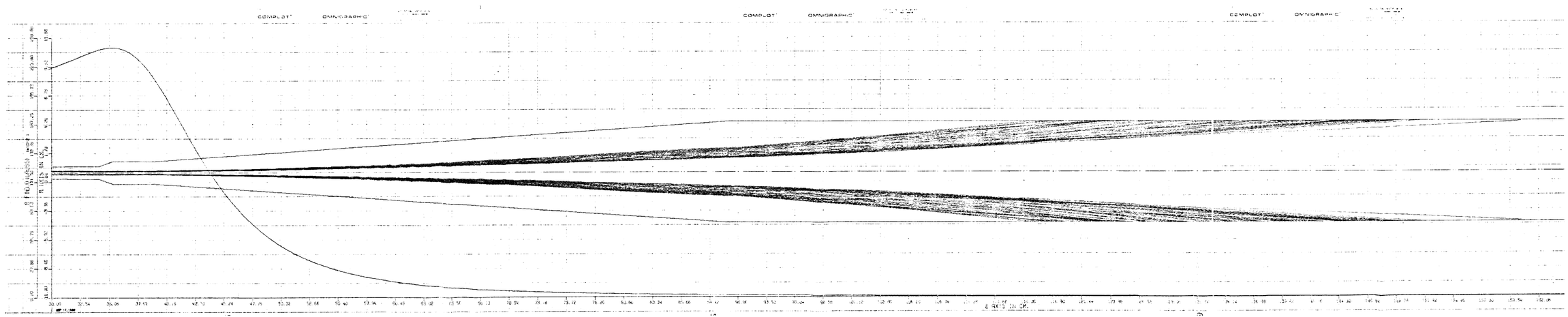
COMPLOT
OMNIGRAPHIC
COMPLOT
OMNIGRAPHIC
COMPLOT
OMNIGRAPHIC

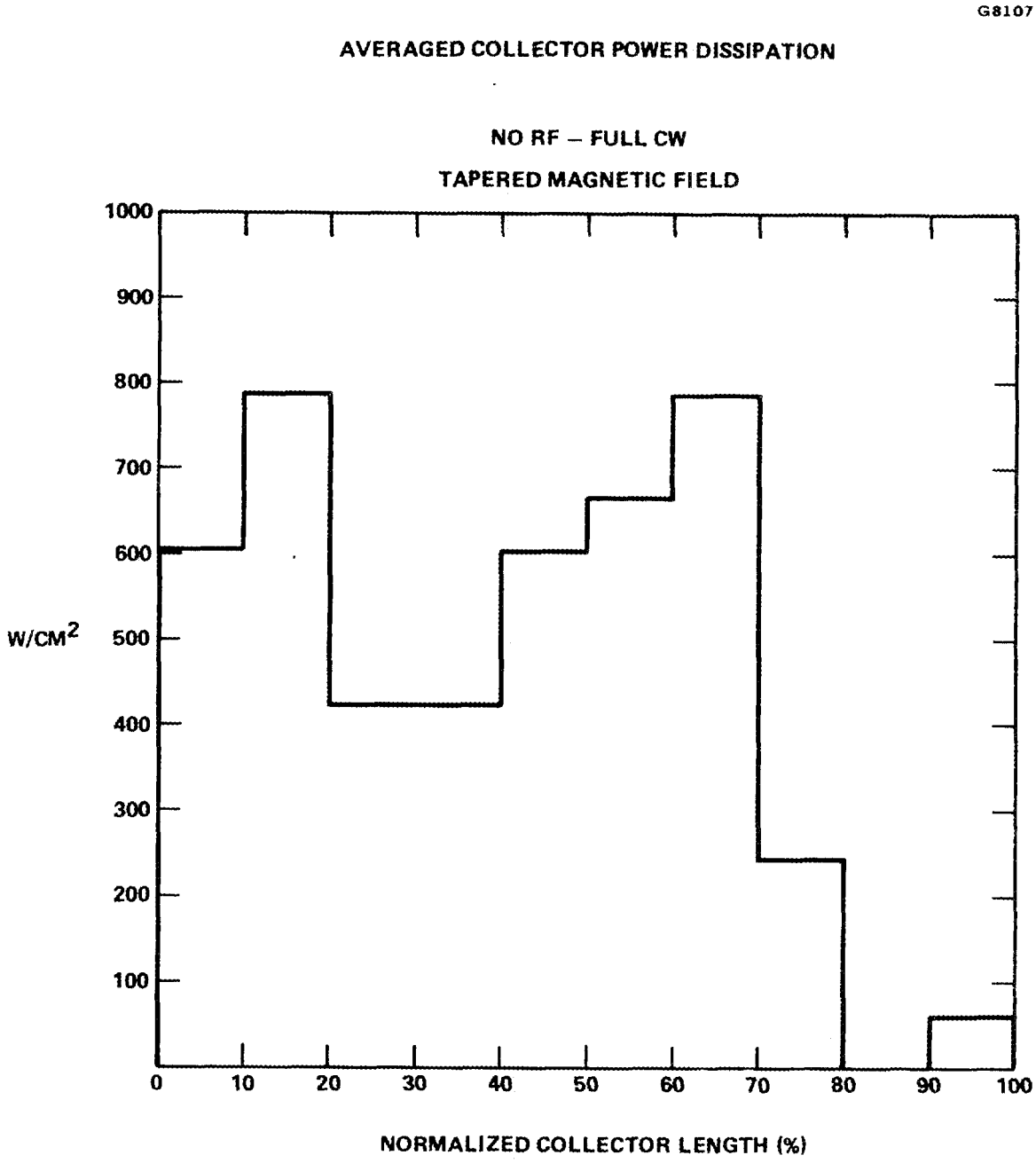


Figure 2.5-4 Averaged power dissipation on the collector, for the trajectory plot of Figure 2.5-3.

the RF exits the cavity region at a diameter of 2 cm (0.787"). After the collector region, the output waveguide system has been established by ORNL to be 6.35 cm (2.5") diameter waveguide.

In order to traverse the region from the cavity to the output, the axisymmetric collector must appear as a circular waveguide system to the RF power. This implies an "up" taper between the cavity and the collector, and a "down" taper between the collector and the output.

An optimum design technique for circular waveguide tapers has been reported by Unger[2]. In the process of evaluating Unger's raised cosine taper for the "down" taper, it was quickly recognized that his assumptions are violated for the case where the start and end radii are both highly overmoded.

It was therefore decided to approach the taper problem from a more fundamental direction. Starting with the classical Telegrapher's transmission line equations, it was determined that these equations could be readily programmed for any waveguide mode, without unnecessary assumptions. Two examples were used to verify program results.

Unger's paper describes a $TE_{01}$ taper designed for 55 GHz, for which the $TE_{02}$ was measured to be attenuated by "greater than 50 dB". When the taper geometry is carefully described as input data to the Taper Computer Program, the result is that the $TE_{02}$ mode is attenuated by more than 62 dB. The actual computer output is from the graphics plotter and is shown in Figures 2.6-1 a, b and c.

Figure 2.6-1a illustrates the raised cosine taper described by Unger and a $TE_{02}$ signal, which is generated within the taper by a $TE_{01}$ signal at the input, to the left. The amplitude of the $TE_{02}$ signal is arbitrarily normallized, but the wavelength is shown accurately in centimeters

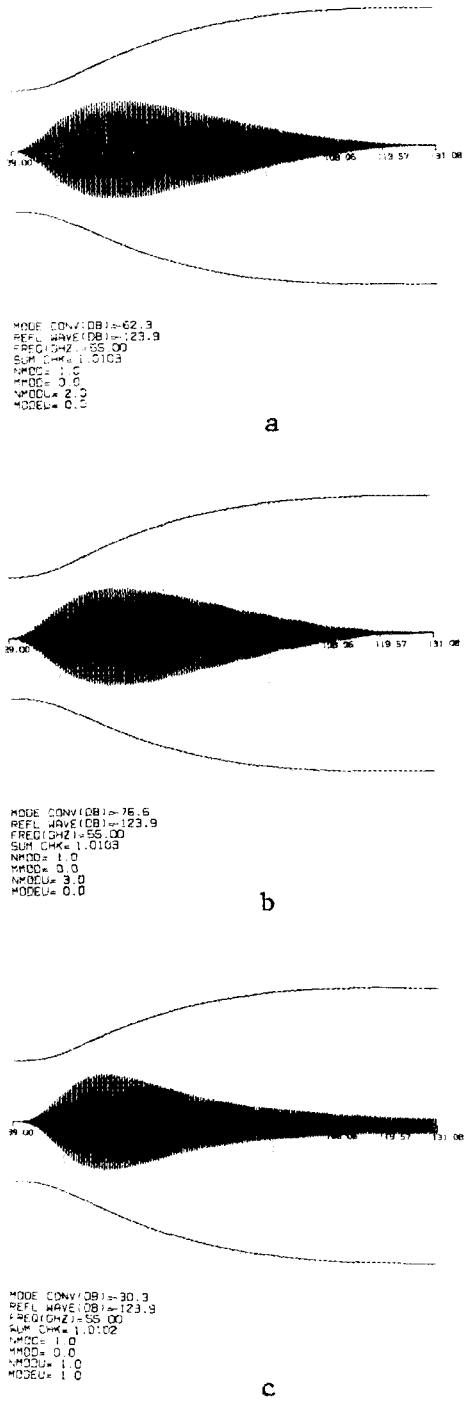


Figure 2.6-1 Unger's raised cosine taper for 55 GHz (Reference 2)

a. $TE_{02}$ mode suppression.

b. $TE_{03}$ mode suppression.

c. $TE_{11}$ mode suppression.

according to the scale along the axis. Figures 2.6-1 b and c illustrate the $TE_{03}$ and $TE_{11}$ modes, respectively, showing 76.6 dB and 30.3 dB mode suppression.

These Figures reveal that for an incident circular waveguide mode, the taper causes RF energy to be transferred and shared among many other modes. Usually the greatest transfer occurs near the beginning of the taper. The goal of an optimized design is to terminate the taper when the greatest amount of energy is in the desired mode.

Another taper that has been employed to verify the accuracy of the Taper Computer Program is one that Hughes EDD has designed for a 94 GHz gyrotron amplifier, operating in the $TE_{01}$ mode. This taper, shown in Figure 2.6-2, must vary from 0.4 cm diameter to 2.6 cm diameter. The taper was derived from Unger's approximate equations to yield 30 dB suppression of the $TE_{02}$ mode. As can be seen in Figure 2.6-2, the computed result is -29.7 dB.

The design of a taper for the 60 GHz gyrotron is restricted to the axial distance between the cavity and collection region (less some arbitrary but finite guard region, so that the beam does not collect on the taper). A 52.5 cm linear taper is depicted in Figure 2.6-3, for an incident $TE_{02}$ mode, and the resulting $TE_{01}$ and $TE_{03}$ mode suppression is on the order of 10 dB.

Figure 2.6-3 also shows that, at an axial point of about 44 cm, $TE_{01}$ and $TE_{03}$ amplitudes approach zero, corresponding to maximum energy in the $TE_{02}$ mode. A designer could stop the taper at this point, continue with a straight waveguide for a short distance, then begin a new linear taper, searching for the next null of the $TE_{01}$ and $TE_{03}$ modes. In this manner, a series of step-tapers could be empirically produced with the computer.

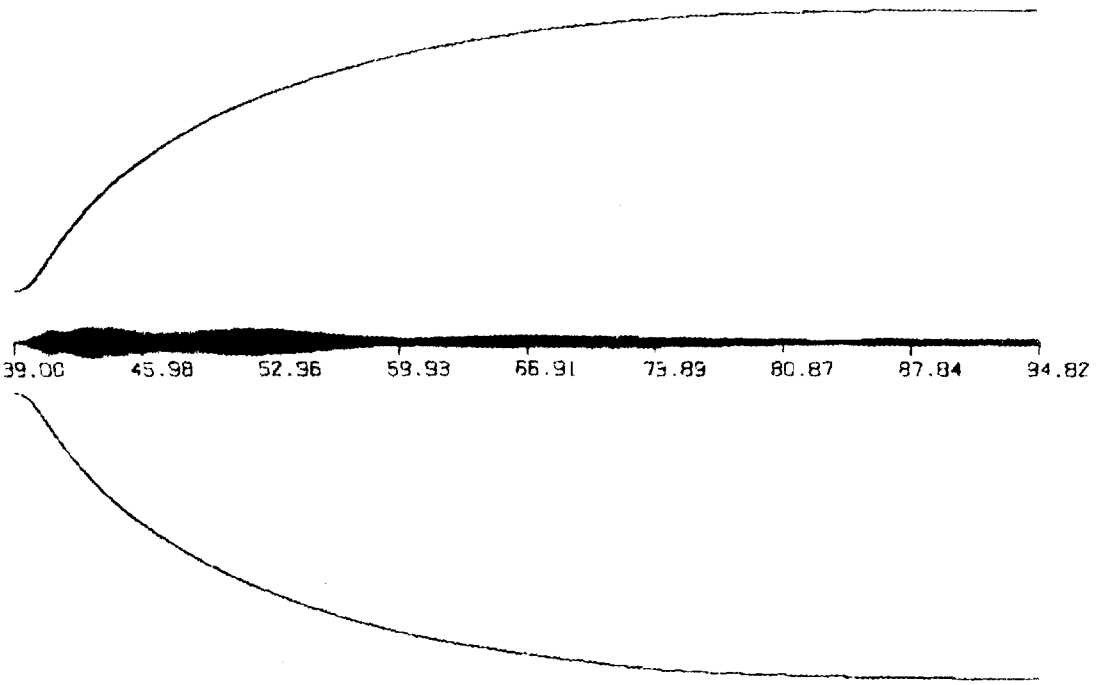


MODE CONV(DB)=-29.7
FREQ(GHZ)=200.00
SUM CHK= 1.2868
NMOD= 1.0
MMOD= 0.0
NMODU= 2.0
MODEU= 0.0

Figure 2.6-2 $TE_{01}$ raised cosine tapper for 94 GHz gyrotron amplifier, with ≈ 30dB suppression of the $TE_{02}$ mode.

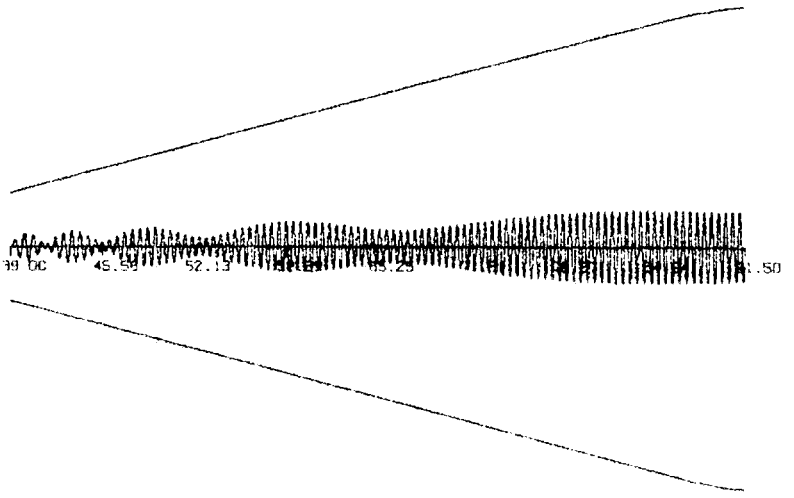


MODE CONV(DB)=-9.8
FREQ(GHZ)=60.00
SUM CHK= 1.0004
NMOD= 2.0
MMOD= 0.0
NMODU= 3.0
MODEU= 0.0

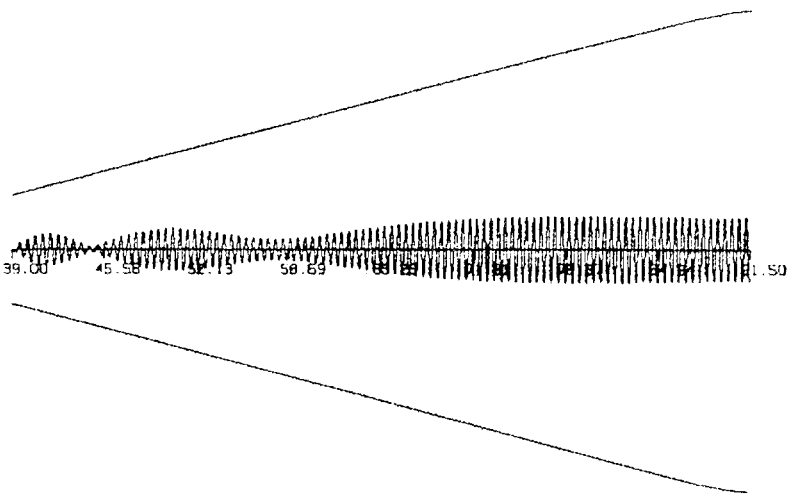


MODE CONV(DB)=-10.8
FREQ(GHZ)=60.00
SUM CHK= 1.0004
NMOD= 2.0
MMOD= 0.0
NMODU= 1.0
MODEU= 0.0

Figure 2.6-3 Linear taper for the ORNL 60 GHz gyrotron.
a. -10.8 dB $TE_{01}$ mode suppression.
b. -9.8 dB $TE_{03}$ mode suppression.

Figure 2.6-4 depicts a raised cosine taper designed for 17 dB $TE_{01}$ mode suppression within a length constraint of 66 cm. An alternative taper configuration, formed empirically from two arcs, is illustrated in Figure 2.6-5, with 20 dB mode suppression.

The "down" taper from 3.5" to 2.5" diameters has proven to be the greater challenge of the two tapers. The raised cosine "down" taper, for instance, was calculated to be twice as long as the "up" taper. The starting diameter of the taper is so large that more than 700 modes could exist in the waveguide. Linear tapers of about 20 cm length were only effective to about 10 dB mode suppression. A variety of other tapers, empirically determined, were moderately more successful. These are shown in Figures 2.6-6 thru 8. Somewhat surprisingly, the best "down" taper was produced by Figure 2.6-8, wherein the taper actually reduces quickly, then increases in diameter for about half its length.

Figure 2.6-9 illustrates the combined "up" taper, collector region and "down" taper. The latter taper is a linear 60 cm taper. The resulting overall mode suppression is of the order of 17 dB. As expected, no energy is exchanged under the straight cylindrical collector region. This 60 cm "down" taper is longer than desired, and some additional effort is required before deciding on the exact "down" taper to be used.

The results of the Taper Computer Program indicate that smoothly varying curved surfaces provide optimum mode suppression. Linearizing a curved surface by dividing the curve into a finite number of linear tapers can deteriorate the mode suppression ability of the smooth taper. Figure 2.6-1, for example, was plotted with 50 points, but when the same taper was plotted with 17 points, mode suppression was changed from -62.3 dB to -40.8 dB. This test demonstrates that the method of fabricating the tapers is very important. In all probability, the taper should be manufactured using numerically-controlled machines.

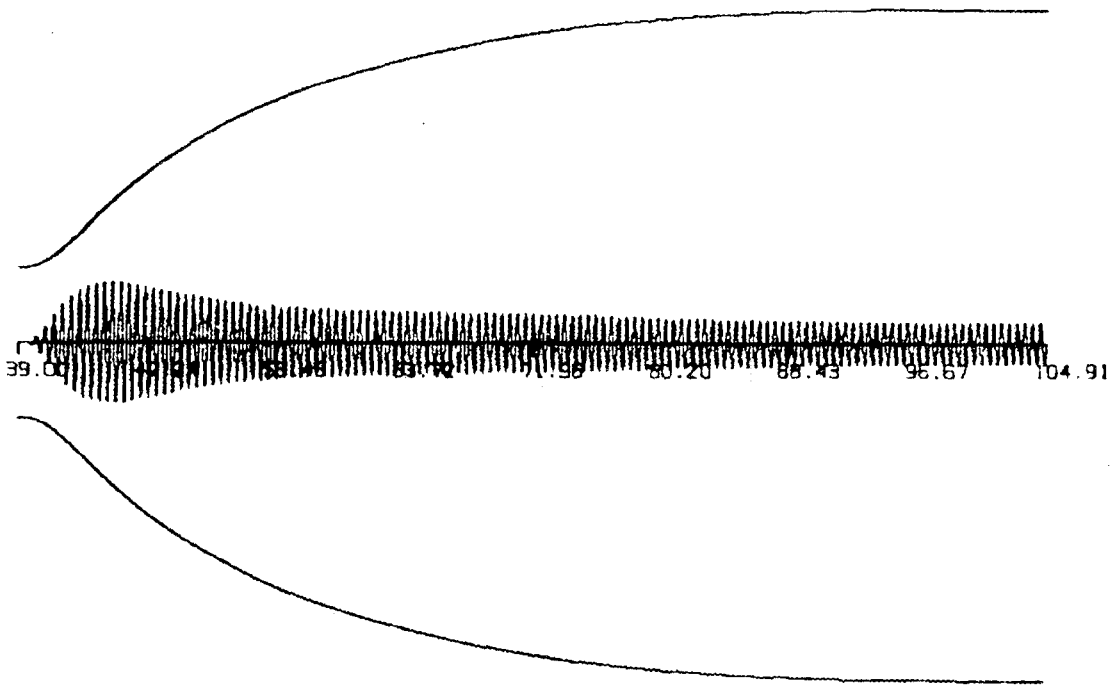


MODE CONV(DB)=-17.3
FREQ(GHZ)=60.00
SUM CHK= 1.0020
NMOD= 2.0
MMOD= 0.0
NMODU= 1.0
MODEU= 0.0

Figure 2.6-4 Raised cosine taper for the ORNL gyrotron, with the $TE_{01}$ mode suppressed 17.3dB.

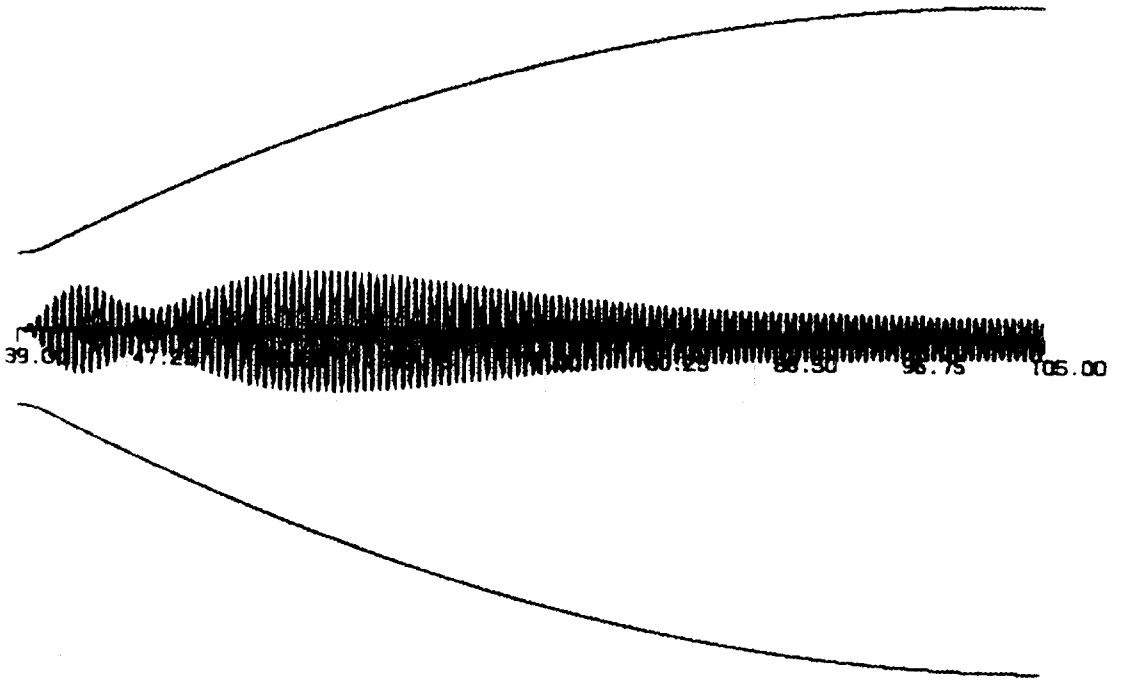


MODE CONV(DB)=-20.1
REFL WAVE(DB)=-200.0
FREQ(GHZ)=62.00
SUM CHK= 1.0011
NMOD= 2.0
MMOD= 0.0
NMODU= 1.0
MODEU= 0.0

Figure 2.6-5 "Two-arc" taper for 20 dB $TE_{01}$ mode suppression in the ORNL gyrotron.

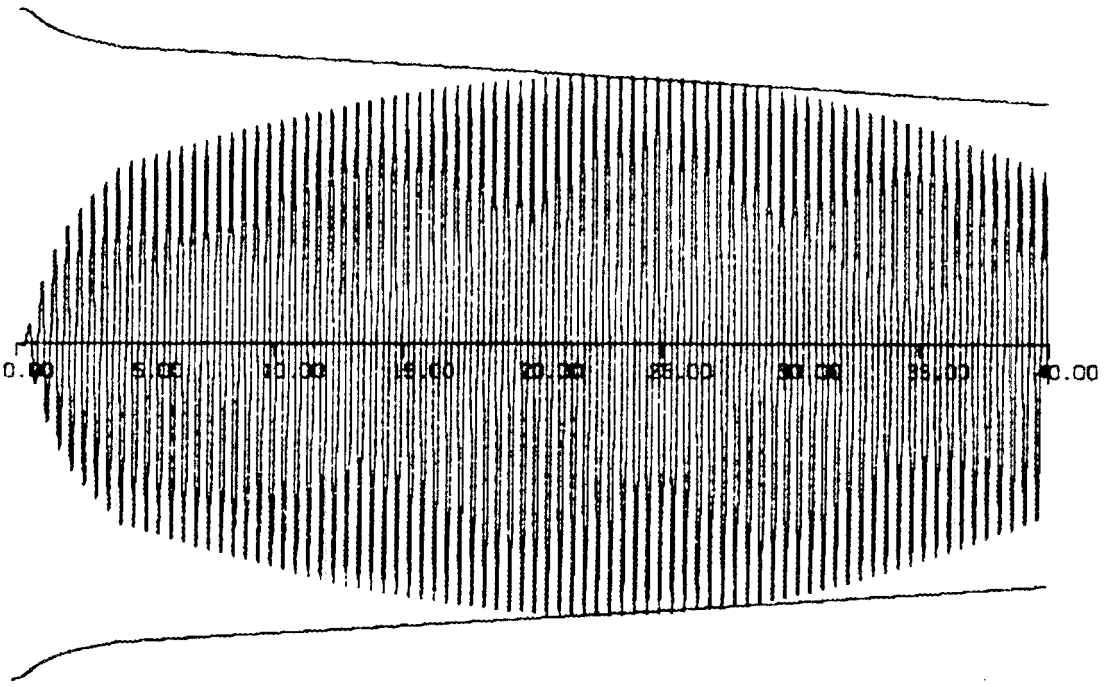


MODE CONV(DB)=-15.0
REFL WAVE(DB)=-200.0
FREQ(GHZ)=62.00
SUM CHK= 1.0009
NMOD= 2.0
MMOD= 0.0
NMODU= 1.0
MODEU= 0.0

Figure 2.6-6 A "two arc/linear" taper of 40 cm length.

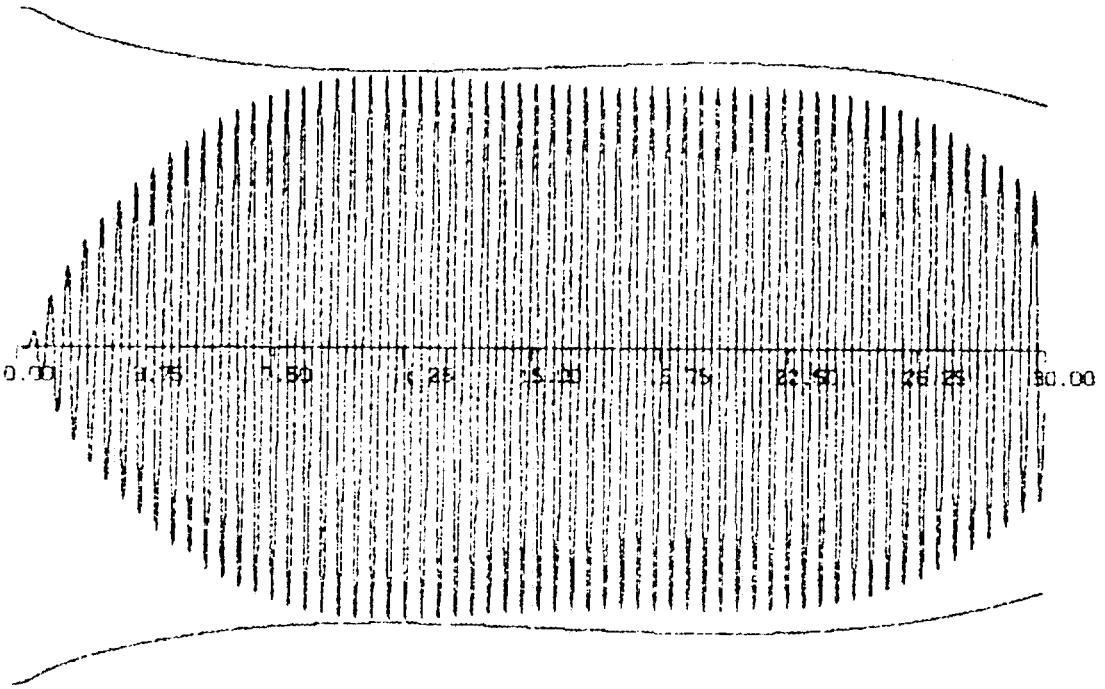


MODE CONV(DB)=-15.4
REFL WAVE(DB)=-200.0
FREQ(GHZ)=62.00
SUM CHK= 1.0003
NMOD= 2.0
MMOD= 0.0
NMODU= 1.0
MODEU= 0.0

Figure 2.6-7 "Two arc" "down" taper of 30 cm length.

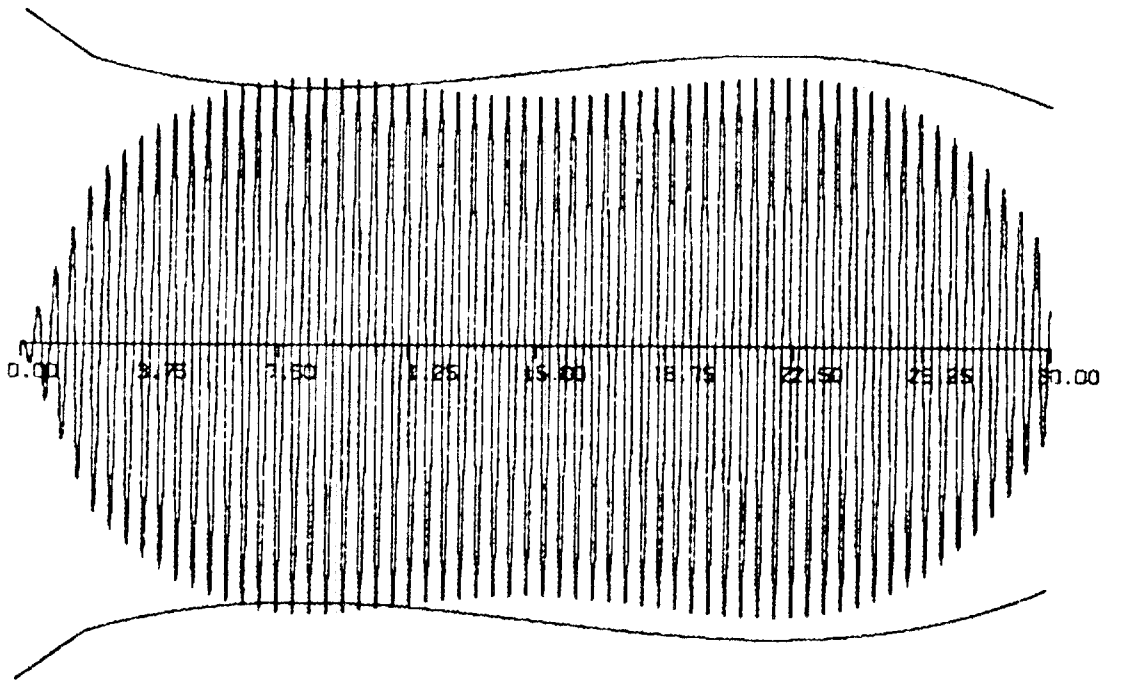


MODE CONV(DB)=-17.7
REFL WAVE(DB)=-200.0
FREQ(GHZ)=62.00
SUM CHK= 1.0003
NMOD= 2.0
MMOD= 0.0
NMODU= 1.0
MODEU= 0.0

Figure 2.6-8 A modified "two arc" taper of 30 cm length.

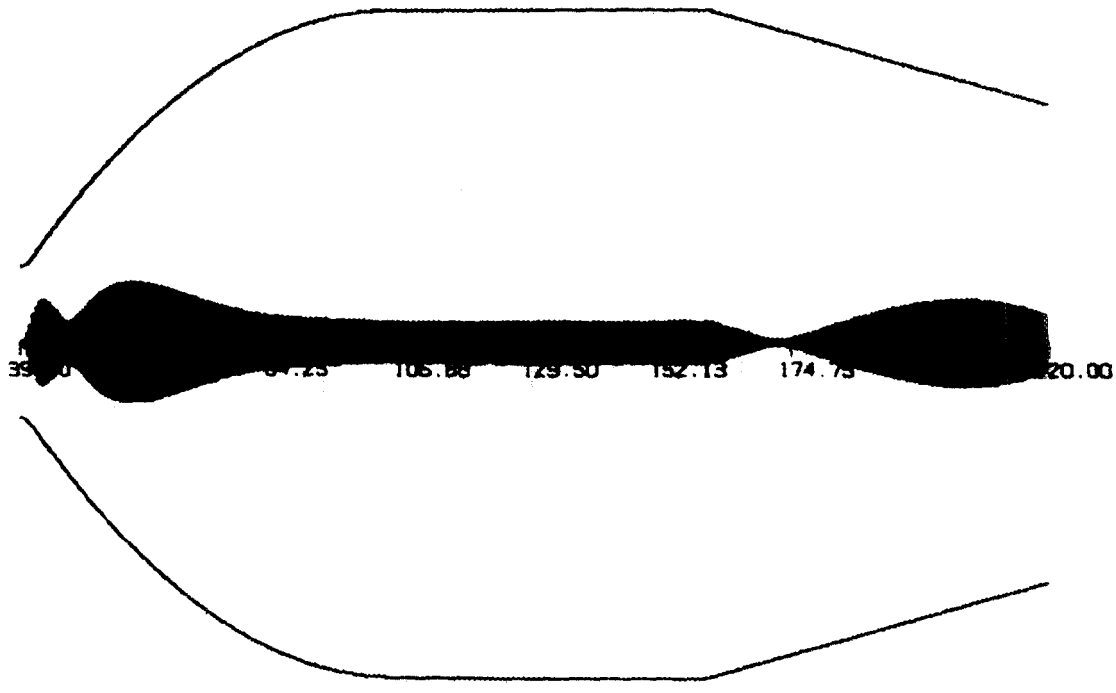


MODE CONV(DB)=-17.1
REFL WAVE(DB)=-200.0
FREQ(GHZ)=62.00
SUM CHK= 1.2446
NMOD= 2.0
MMOD= 0.0
NMODU= 1.0
MODEU= 0.0

Figure 2.6-9 Combined "up" taper, collector region, and "down" taper with 17 dB overall suppression of the $TE_{01}$ mode.

With the Taper Computer Program, Hughes has developed an invaluable tool for assuring that the RF energy from the gyrotron will be delivered to the plasma in the desired mode.

## 2.7 TUBE LAYOUT

Based on the electrical design to date, the preliminary gyrotron layout is as shown in Figure 2.7-1. The total length is 241 cm (94.9").

## 2.8 POWER SUPPLIES

A Hughes team, composed of two EDD plant engineers and two transmitter technicians from the Ground Systems Group were sent to Kwajalein to disassemble the MSR transmitter and cooling system. This effort was completed by mid June.

A Pan American Van Lines representative was sent to Kwajalein to supervise the packing of the disassembled power supply and cooling system. The actual packing is being done by Global Associates, who were turned-on by letter-subcontract from Hughes.

It is uncertain at this time whether the packing can be completed in time for the July barge. If not, the next departure is mid-August.

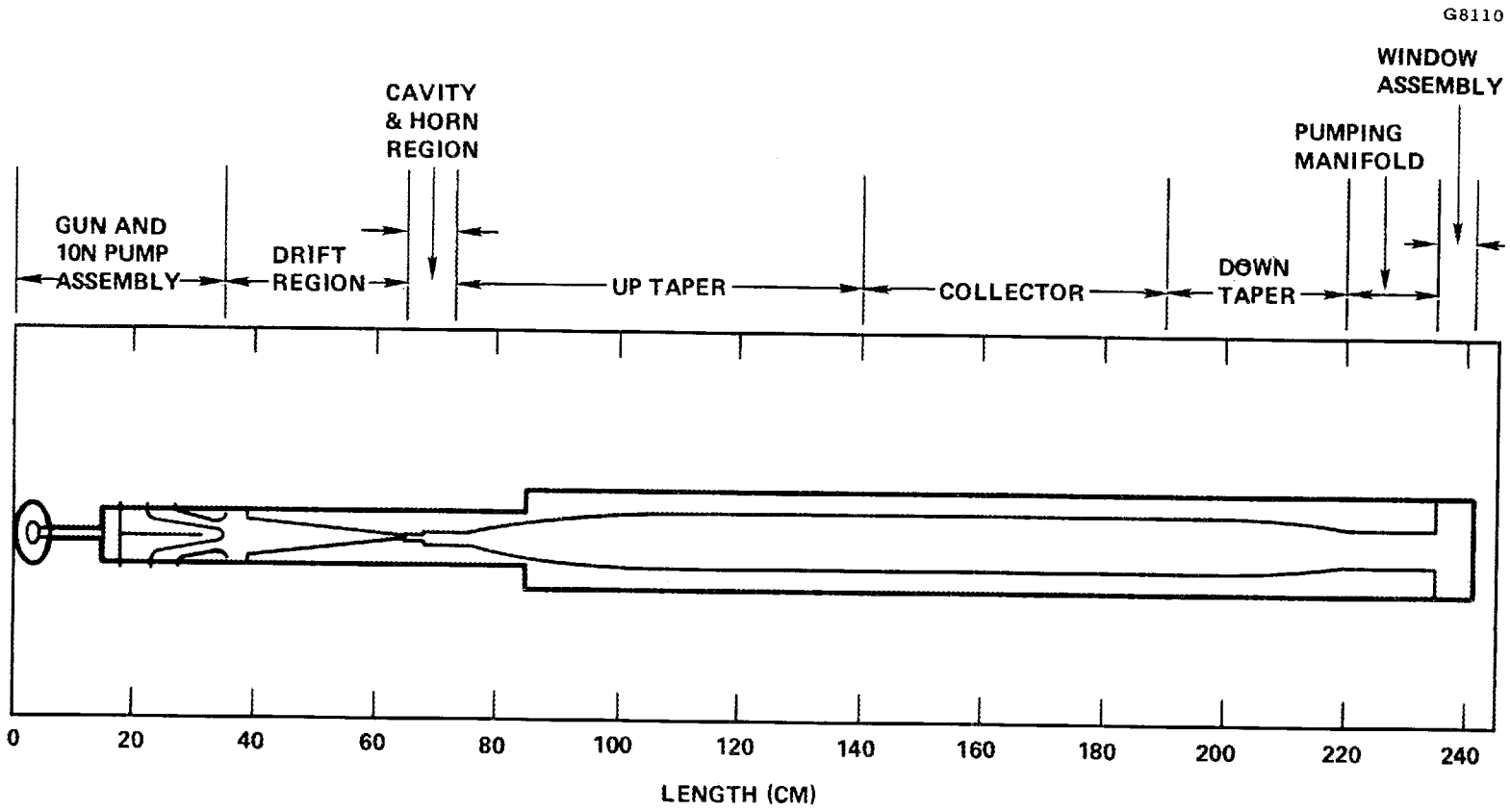


Figure 2.7-1 Preliminary 917H gyrotron layout for ORNL.

## III. SCHEDULE

3.1 A revised program plan is attached which includes greater visibility of the gyrotron development. Page 2 of the schedule encompasses the major facility planning which is required.

The low duty power supply is being furnished by Hughes for diagnostic measurements of the first tubes. A DOE-furnished supply capable of 100 ms pulses, is scheduled to be available by April 1981. Installation and check out of this supply is scheduled to be completed by June 1981.

The reassembly of the Kwajalein supply is dependent upon space availability. The schedule assumes space will be available by October 1980, and the Kwajalein supply reassembly could then be completed by June 1981.

917H 60 GHz 200 KW CW GYROTRON – ORNL CONTRACT NO. W-7405-ENG-26
MILESTONE SCHEDULE AND STATUS REPORT – GYROTRON DEVELOPMENT

AS OF 6/30/80 REVISION DATE _____ SHEET 1 OF 2

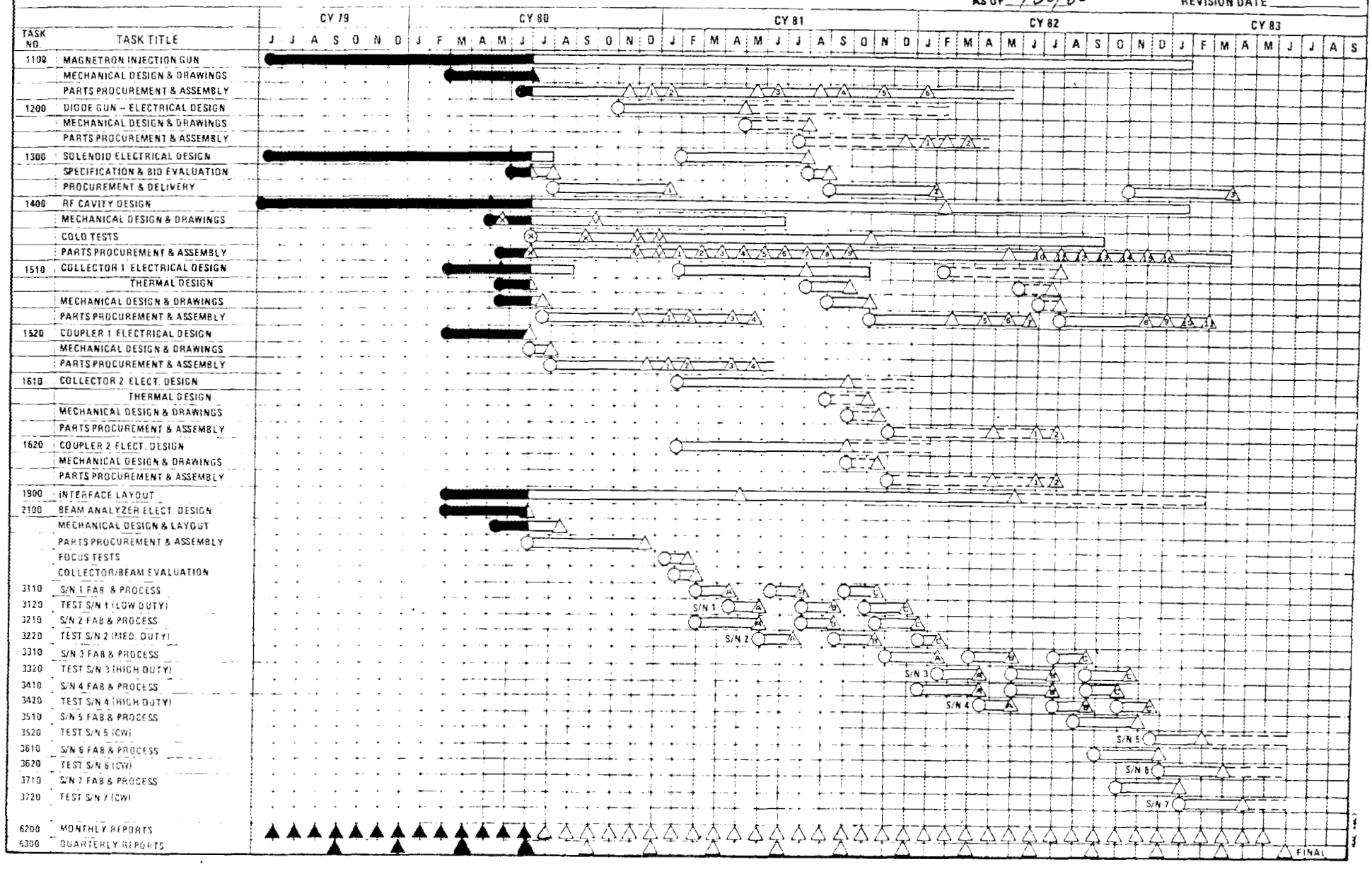

OAK RIDGE NATIONAL LABORATORY GYROTRON DEVELOPMENT PROGRAM
FACILITY MILESTONE SCHEDULE AND STATUS REPORT

AS OF 6/30/80

SHEET 2 OF 2

REVISION DATE

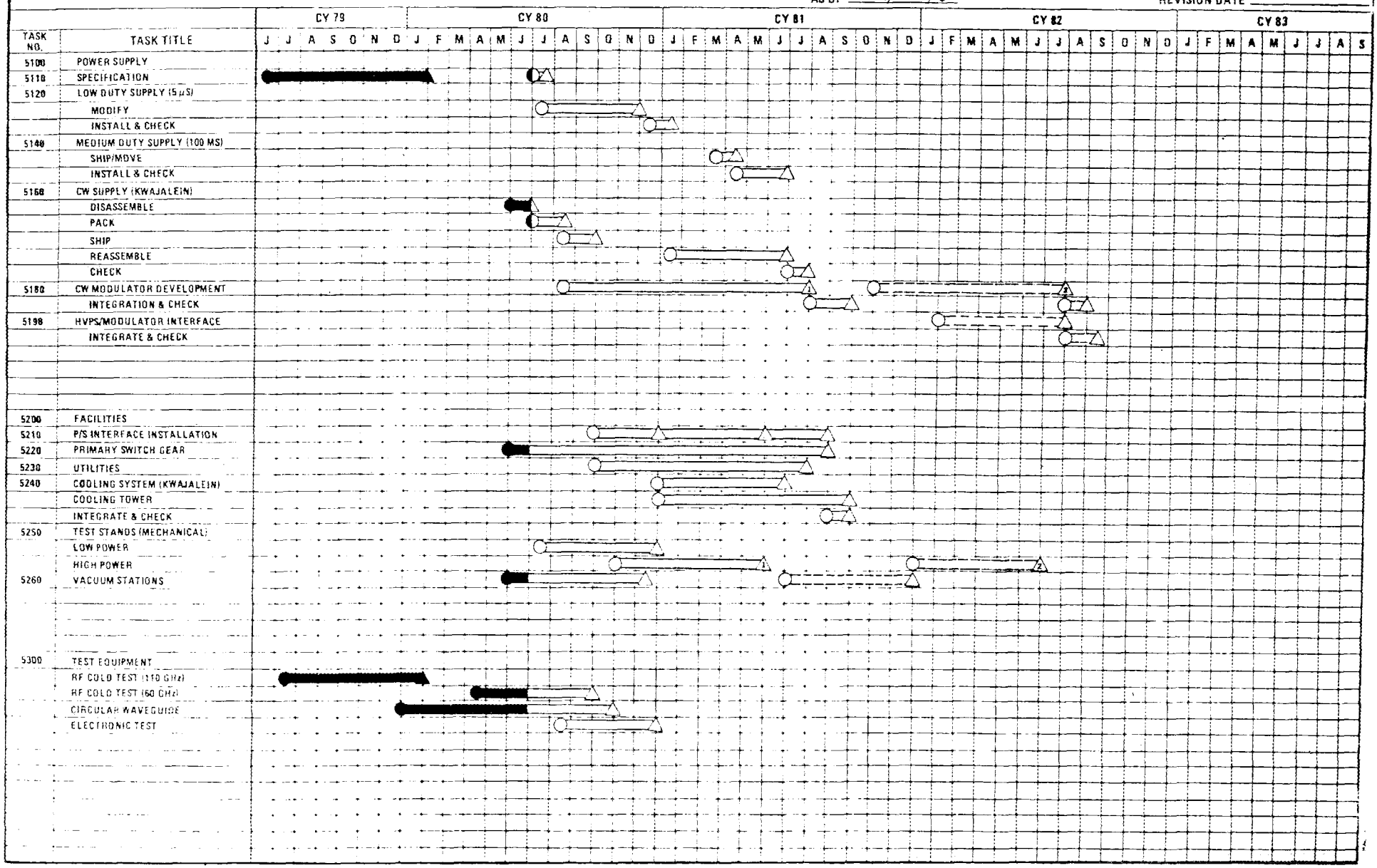

## IV REFERENCES


1. Arnold, K. W., et al, Development Program for a 200 kW, CW Gyrotron, Quarterly Report No. 3, prepared by Hughes Aircraft Company for Oak Ridge National Laboratory under Contract No. W-7405-ENG-26, ORNL/SUB-33200/3, January through March 1980.

2. Unger, H. G., "Circular Waveguide Taper of Improved Design", The Bell System Technical Journal, Vol. 37, July 1958, pp. 899-912.

ORNL/SUB-33200C
7/24/80

## INTERNAL DISTRIBUTION

1. L. A. Berry
2. A. L. Boch
3. J. L. Burke
4. R. J. Colchin
5-8. H. O. Eason
9. O. C. Eldridge
10. R. P. Jernigan
11-12. C. M. Loring
13. H. C. McCurdy
14. O. B. Morgan, Jr.
15. G. F. Pierce
16. T. L. White
17-18. Laboratory Records Department
19. Laboratory Records, ORNL-RC
20. Y-12 Document Reference Section
21-22. Central Research Library
23. Fusion Energy Division Library
24. Fusion Energy Division Communications Center
25. ORNL Patent Office

## EXTERNAL DISTRIBUTION

26. R. A. Dandl, 1122 Calle De Los Serranos, San Marcos, CA 92069
27. A. N. Dellis, Culham Laboratory, Abingdon, Oxon, England, OX143DB
28. W. P. Ernst, Princeton University, Plasma Physics Laboratory, P.O. Box 451, Princeton, NJ 08540
29. W. Friz, AFAL/DHM, Wright Patterson AFB, OH 45433
30. T. Godlove, Particle Beam Program, Office of Inertial Fusion, Department of Energy. Mail Stop C-404, Washington, DC 20545
31. V. L. Granatstein, Naval Research Laboratory, Code 6740, Washington, DC 20375
32. G. M. Haas, Component Development Branch, Office of Fusion Energy (ETM), Department of Energy, Mail Stop G-234, Washington, DC 20545
33. J. L. Hirshfield, Yale University, Department of Engineering and Applied Science, P.O. Box 2159, Yale Station, New Haven, CT 06520
34. H. Ikegami, Institute of Plasma Physics, Nagoya University, Nagoya 464, Japan
35. H. Jory, Varian Associates, 611 Hansen Way, Palo Alto, CA 94303
36. J. V. Lebacqz, Stanford Linear Accelerator Center, P.O. Box 4349, Stanford, CA 94305
37. W. Lindquist, Electronics Engineering Department, Lawrence Livermore Laboratory, P.O. Box 808/L-443, Livermore, CA 94550
38. K. G. Moses, TRW Defense & Space Systems, 1 Space Park, Bldg. R-1, Redondo Beach, CA 90278
39. M. R. Murphy, Office of Fusion Energy (ETM, Department of Energy, Mail Stop G-234, Washington, DC 20545
40. V. B. Napper, Three Dunwoody Park, Suite 112, Atlanta, GA 30341
41. B. H. Quon, TRW Defense & Space Systems, 1 Space Park, Bldg. R-1, Redondo Beach, CA 90278
42. M. E. Read, Naval Research Laboratory, Code 6740, Washington, DC 20375
43. D. B. Remsen, General Atomic Company, P.O. Box 81608, San Diego, CA 92138
44. B. Stallard, Lawrence Livermore Laboratory, University of California, L-437, P.O. Box 808, Livermore, CA 94550
45. H. S. Staten, Office of Fusion Energy (ETM), Department of Energy, Mail Stop G-234, Washington, DC 20545
46. P. Tallerico, AT-1, Accelerator Technology Division, Los Alamos Scientific Laboratory, Mail Stop 817, P.O. Box 1663, Los Alamos, NM 87545

INDEX
3 11/16 PHOTOMASTER (DOUBLE 4 1/16 X 11 5/8 COLUMN)
SECTION FINISH SIZE 8 1/2 X 11 - DOUBLE 3 1/16 X 8 11/16 COLUMN)

EXTERNAL DISTRIBUTION (continued)

47. R. J. Temkin, National Magnet Laboratory, Massachusetts Institute of Technology, Cambridge, MA 02139
48. A. Trivelpiece, Science Applications, Inc., 1200 Prospect Street, P.O. Box 2351, LaJolla, CA 92038
49. Director, U.S. Army Ballistic Missle Defense Advance Technology Center, Attn.: D. Schenk, ATC-R, P.O. Box 1500, Huntsville, AL 35807

50-51. Department of Energy Technical Information Center, Oak Ridge, TN 37830

52. RADC/OCTP, Griffiss AFB, NY 13441
53. Office of Assistant Manager for Energy Research and Development, Oak Ridge Operations Office, Department of Energy, Oak Ridge, TN 37830

INDEX
4 11/16 PHOTOMASTER (DOUBLE 4 1/16 x 11 5/8 COLUMN)
ACTION (FINISH SIZE 8 1/2 x 11 - DOUBLE 3 1/16 x 8 11/16 COLUMN)